



The Chip, Mia and the Table

Lejla Batina

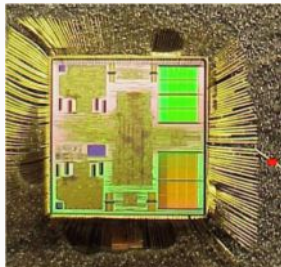
March 4, 2020

Institute for Computing and Information Sciences
Radboud University

High-Tech Women in Science and Technology

March 4, 2020, Darmstadt

The Chip, Mia and the Table



“So, you want to be a cryptographer”, Bruce Schneier’s newsletter, Oct. 1999

Crypto devices



Critical infrastructure, human SCADA systems, IoT devices

CYBERSECURITY VERY WEAK AT CRITICAL DUTCH WATER MANAGEMENT SITES

By Anna Popavie on December 8, 2017 - 10:00



nest



Medical device manufacturer Animas, a subsidiary of Johnson & Johnson, is warning diabetic patients who use its OneTouch Ping insulin pump about security issues that could allow hackers to deliver unauthorized doses of insulin.

Can Hackers Get Into Your Pacemaker?

Lapses in cybersecurity leave hospital records and patients' medical devices open to exploitation.

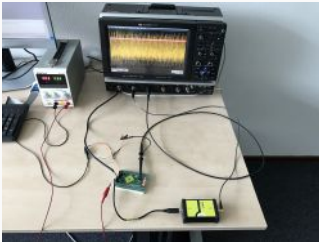


"Broken Hearts": How plausible was the Homeland pacemaker hack?

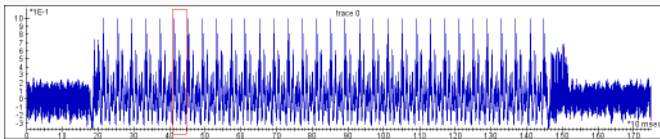
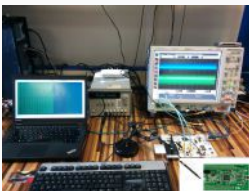
By Barryly Jack (@BarrylyJack)



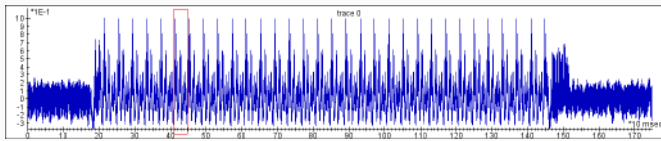
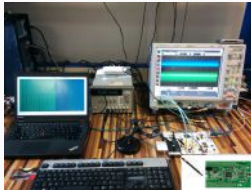
Side-channel attacks



Using physical leakages

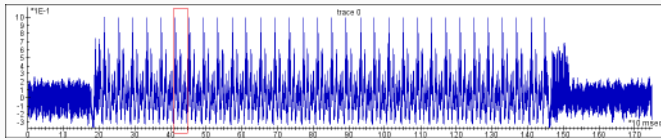


Using physical leakages



- ▶ Recovering secrets through timing, power consumption, EM

Using physical leakages



- ▶ Recovering secrets through timing, power consumption, EM
- ▶ Often, optimizations enable leakages

September 3, 2019



Research Post: Cache Attacks on CTR_DRBG - Forgotten Assumptions
This post presents results from our paper "Pseudorandom Black Swans: Cache Attacks on CTR_DRBG". We illustrate how omissions in...
security.cohnen.info

Relevance

September 3, 2019



Research Post: Cache Attacks on CTR_DRBG - Forgotten Assumptions
This post presents results from our paper "Pseudorandom Black Swans: Cache Attacks on CTR_DRBG". We illustrate how omissions in...
security.cohnen.info

October 3, 2019

Researchers Discover ECDSA Key Recovery Method

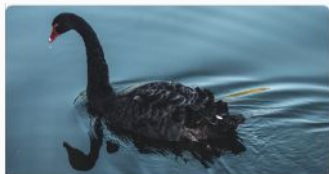


Relevance

November 13, 2019



September 3, 2019



Research Post: Cache Attacks on CTR_DRBG - Forgotten Assumptions
This post presents results from our paper "Pseudorandom Black Swans: Cache Attacks on CTR_DRBG". We illustrate how omissions in...
security.cohney.info

October 3, 2019

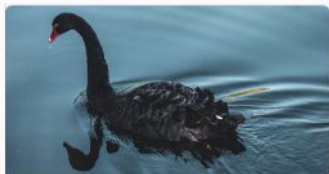
Researchers Discover ECDSA Key Recovery Method



November 13, 2019



September 3, 2019



Research Post: Cache Attacks on CTR_DRBG - Forgotten Assumptions
This post presents results from our paper "Pseudorandom Black:
Swans: Cache Attacks on CTR_DRBG". We illustrate how omissions in...
security.cohnen.info

October 3, 2019

Researchers Discover ECDSA Key Recovery Method



December 12, 2019

PUNDITVAULT — Intel's SGX coughs up crypto keys when scientists tweak CPU voltage

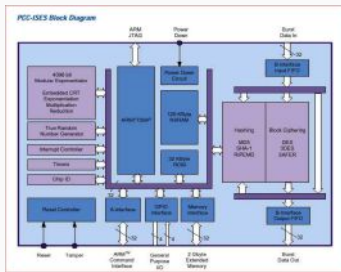
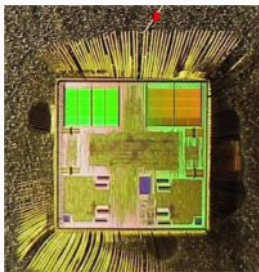
Install fees when they become available. Until then, don't sweat it.

By [David Kanter](#) • December 12, 2019



The chip

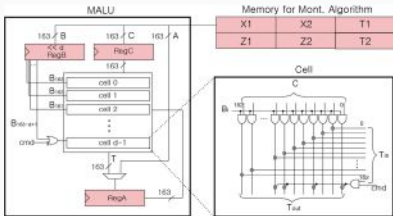
An RSA crypto chip of Pijnenburg Securealink cca year 2000



The chip featured:

- ▶ Modular exponentiator for RSA (2 units, up to 2048 bit)
 - ▶ Symmetric crypto: (3)DES, SAFER
 - ▶ Hashing: MD5, SHA1 and RIPEMD
 - ▶ True Random Number Generator

ECC RFID chip 2007



MIT News
INNOVATION ACROSS THE WORLD

Energy-efficient encryption for the internet of things

Special-purpose chip reduces power consumption of public-key encryption by 99.75 percent, increases speed 500-fold.

Larry Hardesty | MIT News Office
February 12, 2018

Press Inquiries
617.253.1737

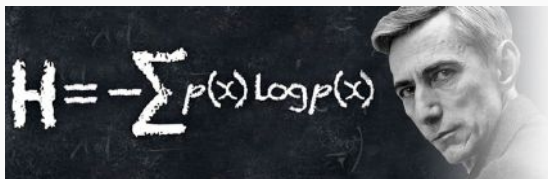
- ▶ Several protocols were designed for different RFID applications
- ▶ ECC co-processor that can compute:
 - ECC scalar multiplications
 - finite field operations
- ▶ Schnorr protocol: one scalar multiplication
 - 14K gates, 79K cycles
 - 30 μ Watt@500 KHz and performance of 158 msec
 - energy of 4.8 μ Joule

MIA

Information theoretic approach to side-channel analysis

Started cca 2006

- ▶ MIA was proposed as a new SCA distinguisher
- ▶ started a new line of research into information theoretic view to side-channel analysis



We introduce a Mutual Information-based distinguisher that constitutes the core of a new and generic differential side-channel attack: Mutual Information Analysis (MIA). In contrast to [17], we apply information theory to develop a powerful attack without any device characterization. The distinguisher uses only

MIA and the chip: Location-based leakage

- ▶ Registers, memory and other storage units exhibit identifiable and data-related leakage

- ▶ Registers, memory and other storage units exhibit identifiable and data-related leakage when accessed
- ▶ Exploit dependence between the secret key and the location of the activated component

- ▶ Registers, memory and other storage units exhibit identifiable and data-related leakage when accessed
- ▶ Exploit dependence between the secret key and the location of the activated component

Algorithm 3: Montgomery ladder

Input: $P, k = (k_{x-1}, k_{x-2}, \dots, k_0)_2$

Output: $Q = k \cdot P$

$R_0 \leftarrow P$

$R_1 \leftarrow 2 \cdot P$

for $i = x - 2$ **downto** 0 **do**

$b = 1 - k_i$

$R_b = R_0 + R_1$

$R_{k_i} = 2 \cdot R_{k_i}$

end for

return R_0

- ▶ Sugawara et al. considered so-called “geometric” leakage in an ASIC

- ▶ Sugawara et al. considered so-called “geometric” leakage in an ASIC
- ▶ Heyszl et al. recovered the secret scalar by exploiting the spatial dependencies of the double-and-add-always algorithm for ECC on FPGA

- ▶ Sugawara et al. considered so-called “geometric” leakage in an ASIC
- ▶ Heyszl et al. recovered the secret scalar by exploiting the spatial dependencies of the double-and-add-always algorithm for ECC on FPGA
- ▶ Schlosser et al. use photonic side-channel to recover the exact SRAM location accessed during the activation of an AES S-box lookup table

- ▶ Sugawara et al. considered so-called “geometric” leakage in an ASIC
- ▶ Heyszl et al. recovered the secret scalar by exploiting the spatial dependencies of the double-and-add-always algorithm for ECC on FPGA
- ▶ Schlosser et al. use photonic side-channel to recover the exact SRAM location accessed during the activation of an AES S-box lookup table
- ▶ Algorithmic countermeasures such as register renaming were considered

- ▶ Sugawara et al. considered so-called “geometric” leakage in an ASIC
- ▶ Heyszl et al. recovered the secret scalar by exploiting the spatial dependencies of the double-and-add-always algorithm for ECC on FPGA
- ▶ Schlosser et al. use photonic side-channel to recover the exact SRAM location accessed during the activation of an AES S-box lookup table
- ▶ Algorithmic countermeasures such as register renaming were considered
- ▶ Literature sometimes referred to those as address attacks

- ▶ Sugawara et al. considered so-called “geometric” leakage in an ASIC
- ▶ Heyszl et al. recovered the secret scalar by exploiting the spatial dependencies of the double-and-add-always algorithm for ECC on FPGA
- ▶ Schlosser et al. use photonic side-channel to recover the exact SRAM location accessed during the activation of an AES S-box lookup table
- ▶ Algorithmic countermeasures such as register renaming were considered
- ▶ Literature sometimes referred to those as address attacks

- ▶ Distinguishing the activity of small regions

- ▶ Distinguishing the activity of small regions
- ▶ Exploiting the spatial dependencies of crypto algorithms

- ▶ Distinguishing the activity of small regions
- ▶ Exploiting the spatial dependencies of crypto algorithms
- ▶ Forward Neural Networks classifiers exploiting location-based side-channel on the SRAM of a ARM Cortex-M4

- ▶ Distinguishing the activity of small regions
- ▶ Exploiting the spatial dependencies of crypto algorithms

- ▶ Forward Neural Networks classifiers exploiting location-based side-channel on the SRAM of a ARM Cortex-M4
- ▶ 2 SRAM regions of 128 bytes each can be distinguished with 100% success rate and 256 SRAM byte-regions with 32% success rate

- ▶ Implementation of a key-dependent crypto operation using certain storage components in a deterministic way e.g. a lookup-table (AES LUT)

- ▶ Implementation of a key-dependent crypto operation using certain storage components in a deterministic way e.g. a lookup-table (AES LUT)
- ▶ Location leakage is caused by switching circuitry and is observable via EM emissions on the die surface

- ▶ Implementation of a key-dependent crypto operation using certain storage components in a deterministic way e.g. a lookup-table (AES LUT)
- ▶ Location leakage is caused by switching circuitry and is observable via EM emissions on the die surface
- ▶ Adversary aims to infer which part of the table is active

- ▶ Implementation of a key-dependent crypto operation using certain storage components in a deterministic way e.g. a lookup-table (AES LUT)
- ▶ Location leakage is caused by switching circuitry and is observable via EM emissions on the die surface
- ▶ Adversary aims to infer which part of the table is active
- ▶ Adversary uncovers the location information leading to key recovery

Experimental setup



Figure: Modified Pinata ARM STM32F417IG device.

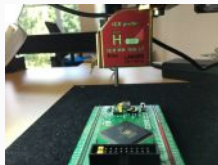


Figure: Decapsulated Pinata with Langer microprobe on top.

Setup details

- ▶ Decapsulated Piñata with ARM Cortex-M4 in 90 nm technology
- ▶ ICR HH 100-27 Langer microprobe $d = 100\mu m$
- ▶ Rectangular grid of 300×300 measurement spots
- ▶ Sampling rate of 1 Gs/sec resulting in 170k samples
- ▶ Near-field probe with positioning accuracy of $50\mu m$
- ▶ Sequential accesses to a cont. region of 16 KBytes in the SRAM using ARM assembly

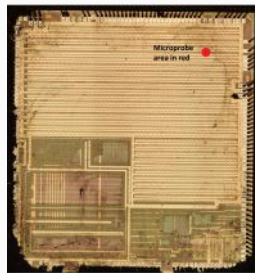


Figure: ARM Cortex-M4 after removal of the plastic layer.

Experiment

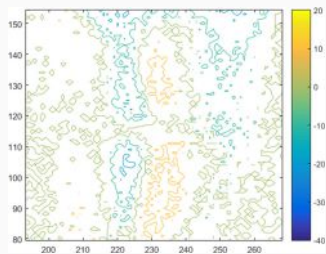


Figure: Distinguishing two 8 KByte regions of the SRAM. Yellow region = stronger leakage from class 1, blue = stronger from class 2.

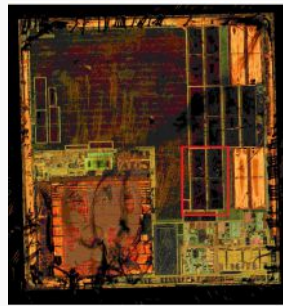
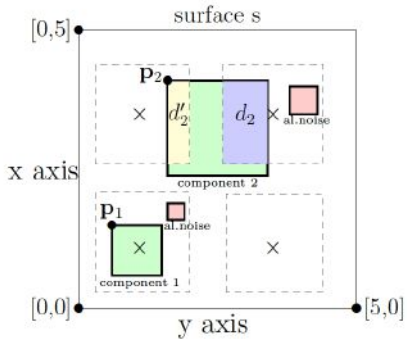


Figure: Red rectangle shows the location where the highest differences were observed.

Parameters

Parameter	Description	Unit	Our example
S	chip surface area	u^2	$\leq 6 \text{ mm}^2$ (whole chip)
O	probe area	u^2	0.03 mm^2
G	scan grid dimension	—	300
A	component areas	vector with 1D entries	—
P	component positions	vector with 2D entries	—

Location Leakage Model



$$l_{[x,y]}^{det} | \mathbf{v}^i = \begin{cases} 0, & \text{if comp. } i \text{ is not captured at } [x,y] \\ d_i, & 0 < d_i < a_i, \text{ if comp. } i \text{ is partially captured at } [x,y] \\ a_i, & \text{if comp. } i \text{ is fully captured at } [x,y] \end{cases}$$

Figure: Vectors $\mathbf{p}_1, \mathbf{p}_2$ show the position of two components whose areas (a_1, a_2) are solid black-line rectangles.

Perceived information metric

$$PI(\mathbf{L}; R) = H[R] - H_{true, model}[\mathbf{L}|R] = H[R] + \sum_{r \in \mathcal{R}} Pr[r] \int_{\mathbf{l} \in \mathcal{L}^{g^2}} Pr_{true}[\mathbf{l}|r] \cdot \log_2 Pr_{model}[r|\mathbf{l}] d\mathbf{l}$$

where $Pr_{model}[r|\mathbf{l}] = \frac{Pr_{model}[\mathbf{l}|r]}{\sum_{r^* \in \mathcal{R}} Pr_{model}[\mathbf{l}|r^*]}$, $Pr_{true}[\mathbf{l}|r] = \frac{1}{n_{test}}$, n_{test} test set size

(1)

Experiment 1: Grid partitioning and dimension

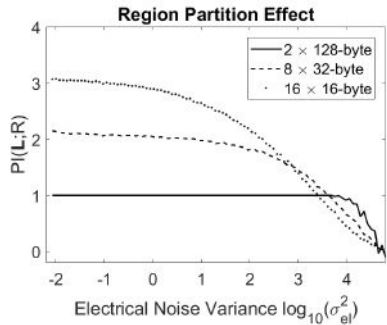


Figure: Effect of 256-byte LUT partitioning to 2, 8 and 16 regions. $\epsilon = \{6 \text{ mm}^2, 0.03 \text{ mm}^2, 100, 92 \mu\text{m}^2, \text{random}\}$

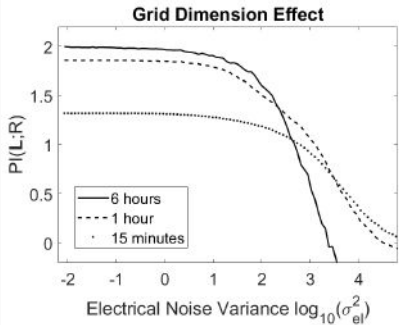


Figure: Effect of grid dim. $g = 100, 40$ and 20 . $\epsilon = \{6 \text{ mm}^2, 0.03 \text{ mm}^2, g, 92 \mu\text{m}^2, \text{random}\}$.

Experiment 2: Technology scaling and algorithmic noise

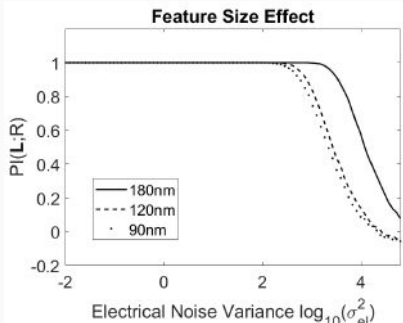


Figure: Feature size of 180 nm, 120 nm, 90 nm and word area $a = 368 \mu m^2, 163 \mu m^2, 92 \mu m^2$. Parameters $\epsilon = \{6 mm^2, 0.03 mm^2, 40, a, \text{random}\}$, 2 x 128 bytes, 250 meas. per spot for 400k traces.

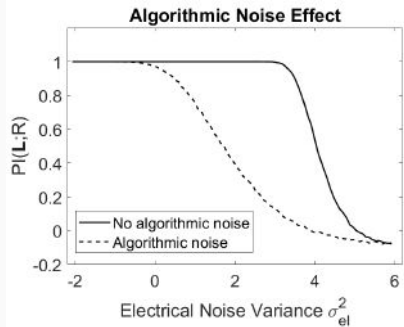


Figure: Alg. noise using 10 noise-generating words. Parameters $\epsilon = \{6 mm^2, 0.03 mm^2, 40, 92 \mu m^2, \text{random}\}$, 2 x 128 bytes, 250 meas. per spot for 400k traces.

Experiment 3: Region proximity and interleaving

- (1) Distant placement: $\approx 1 \text{ mm}$ between 2 regions
- (2) Close placement: the two regions are adjacent to each other.
- (3) Interleaved placement: words of two regions are interleaved

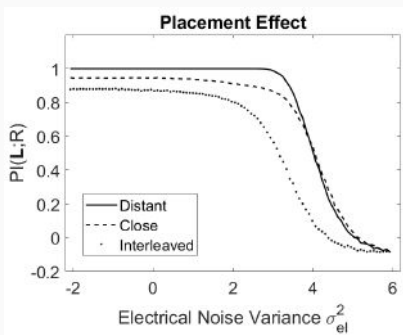
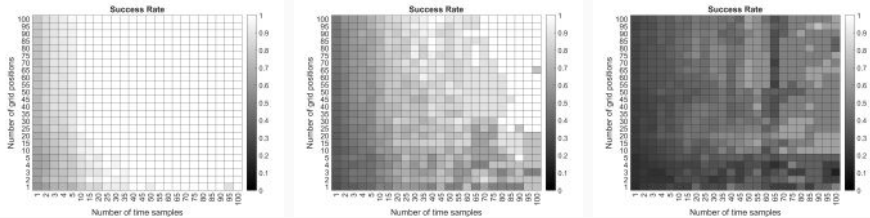


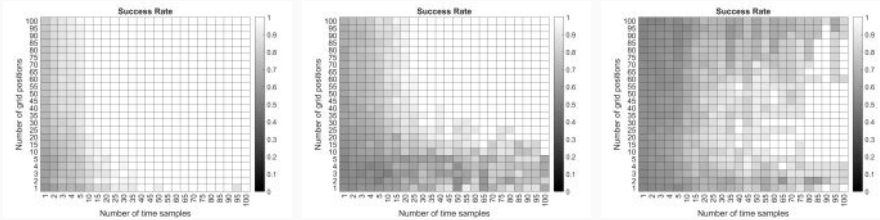
Figure: Effect of different placements. $\epsilon = \{6 \text{ mm}^2, 0.03 \text{ mm}^2, 20, 92 \mu\text{m}^2, \text{random}\}$, 2×128 bytes and using 250 meas. per spot for a total of 100k traces.

Real experiment 1: Region partition



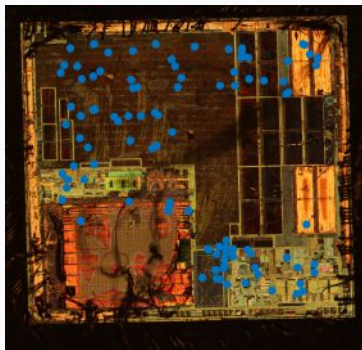
Success rate for template attacks on AES LUT (2x128, 4x64, 8x32). Y-axis denotes # spatial POIs, X-axis denotes # time samples. White – 100% SR and black – 0% SR.

Real experiment 2: Grid dimension



Considered full 300×300 grid (2-day exp.) and scaled down to 40×40 (1-hour) and 10×10 (2-minutes). The theoretical model is unable to classify correctly.

Real experiment 2: Model limitations



Can we do better?

- ▶ Machine learning (ML) proved its potential for SCA

- ▶ Machine learning (ML) proved its potential for SCA
- ▶ ML used for finding POIs, profiling and non-profiling attacks, pre-processing etc.

- ▶ Machine learning (ML) proved its potential for SCA
- ▶ ML used for finding POIs, profiling and non-profiling attacks, pre-processing etc.
- ▶ Deep learning (DL) found suitable in dealing with countermeasures

- ▶ Machine learning (ML) proved its potential for SCA
- ▶ ML used for finding POIs, profiling and non-profiling attacks, pre-processing etc.
- ▶ Deep learning (DL) found suitable in dealing with countermeasures
- ▶ Rapid hardware advances facilitate deep learning

- ▶ Popular pre-trained networks Convolution Neural Network (CNN) classifier
- ▶ Experiments with 2 closely placed SRAM regions of 128 bytes each
- ▶ Single-trace attacks improved compared to templates
- ▶ All 5 CNNs were trained in 2 ways: one batch and multiple-batch training
- ▶ Keras framework and Python for pre-processing
- ▶ Training, validation and test sets are of 70-20-10 ratio

Experiment with CNNs

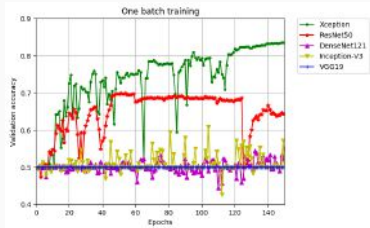


Figure: Single-batch training.

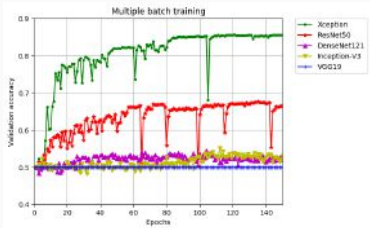


Figure: Multiple-batch training.

CNNs are surpassing the single-sample accuracy of template attacks, reaching 88%.

C. Andrikos, L. Batina, L. Chmielewski, L. Lerman, V. Mavroudis, K. Papagiannopoulos, G. Perin, G. Rassias, A. Sonnino: *Location, Location, Location: Revisiting Modeling and Exploitation for Location-Based Side Channel Leakages*. ASIACRYPT (3) 2019: 285-314.

The Table

Gender diversity: Facts

- ▶ Women are underrepresented in leadership positions
- ▶ Women Need To 'Sit At The Table', Sheryl Sandberg

2015: with 17% of Dutch professors being female, The Netherlands had the fourth-lowest percentage of female professors in Europe

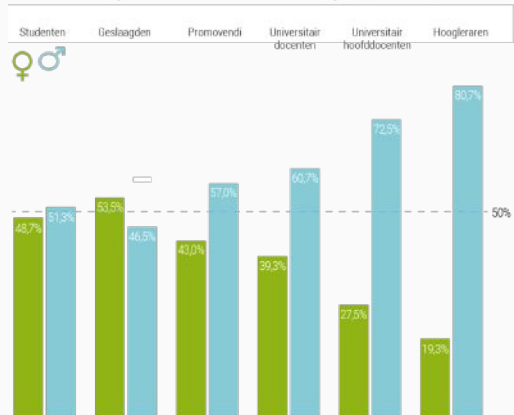
Navratilova: BBC pays McEnroe 10 times more for Wimbledon role

Tennis champion says fellow pundit John McEnroe earns at least £150,000, while she is paid £15,000



Percentages in Dutch academia

Grafiek 2.3 Percentage vrouwen en mannen van student tot hoogleraar (ultimo 2016)



Bron studenten en geslaagden: TcHO 2016, 1 oktober 2016, in personen.

Exclusief wetenschapsgebied Gezondheid

Bron personeel: VSNU/WOP! ultimo 2016, in fte. Exclusief wetenschapsgebied Gezondheid

Initiatives and highlights

- ▶ Gender Diversity committee was formed at Radboud University within the Faculty of Science
- ▶ University-wide mentoring program for women
- ▶ Mohrmann fellowships for women
- ▶ The Radboud Women of Computing Science (RWoCS) group was created: the main goal is to attract female students



- ▶ The chip: Post-quantum crypto for future embedded systems

- ▶ The chip: Post-quantum crypto for future embedded systems
- ▶ MIA: Deep learning for advanced security evaluation

- ▶ The chip: Post-quantum crypto for future embedded systems
- ▶ MIA: Deep learning for advanced security evaluation
- ▶ The Table: More diversity at all entry points

- ▶ The chip: Post-quantum crypto for future embedded systems
- ▶ MIA: Deep learning for advanced security evaluation
- ▶ The Table: More diversity at all entry points



Foto: ANP

Meisjes op havo, vwo en mbo kiezen vaker voor
technische richting

Gepubliceerd: 11 april 2016 23:59

Laatste update: 12 april 2016 07:30



Thank you

We are looking for students/PostDocs!

lejla@cs.ru.nl